ISSN 0036-0244, Russian Journal of Physical Chemistry A, 2014, Vol. 88, No. 11, pp. 2012–2017. © Pleiades Publishing, Ltd., 2014.

PHOTOCHEMSIRTY AND MAGNETOCHEMISTRY

Study on the Growth, Defects, and Optical Properties of Tm:YAP Crystal[1]

Fanming Zeng[a], Dongyang Zheng[a], Chun Li[a]*, Ying Zhang[b], Lin Hai[a], Xiyan Zhang[a], and Jinghe Liu[a]

[a] *Optoelectronic Functional Materials Research Center of the Ministry of Education, Changchun University of Science and Technology, Changchun, 130022 PR China*

[b] *Changchun Institute of Optics, Fine Mechanics and Physics, Chinese Academy of Sciences, Changchun, 130033 PR China*

**e-mail: lichun1210@163.com*

Received December 11, 2013

Abstract—Tm:YAP crystal was grown by the Czochralski method. Color center absorption phenomenon is significantly weakened in the ultraviolet and visible region. Dominated forced convection or increased crystal diameter may reduce the crystal-like scattering dispersion. The average value of absorption coefficient and cross-section are calculated to be 2.09 cm^{-1} and 6.03×10^{-21} cm^2, respectively. The described techniques may be useful for the further improvement of the quality of Tm:YAP crystals.

Keywords: Tm:YAP crystal, crystal annealing, crystal defects, spectral analysis.

DOI: 10.1134/S0036024414110077

Rare-earth ions doped crystals are increasingly important as an active media for solid-state lasers which efficiently are operated under diode pumping. Tm^{3+}-based lasers emitting in the wavelength region of 2 μm are interesting for a large number of application fields such as eye-safe compact devices for DIAL measurements, plastic welding, high-resolution spectroscopy, telecommunications and medical applications [1–3].

The line width of Tm^{3+} ion's $^3F_4 \longrightarrow {}^3H_6$ transition corresponds to the wavelength range of 2 μm, which is similar to the Ho^{3+} ion's $^5I_7 \longrightarrow {}^5I_8$ transition, but the absorption range is wide and the absorption cross-section is large. It is very beneficial to the application in cheap commercial LD pump source, and thus researchers generally use crystal singly doped with Tm^{3+} to produce near 2 μm lasers [4–6].

At present, Nd:YAP crystal had been grown by Li Gansheng et al. [7] from Fujian Institute of Matter and Structure, using the rich yttrium method, with raw material in addition to carbon and natural cooling vacuum method. The Tm:YAP crystal with the size of ∅25 mm × 105 mm had been grown by Czochralski method and characterized by Lu Yanling et al. [8] from Shanghai Jiao Tong University. Mo Xiaogang et al. [9] from Beijing Co. Ltd had grown ∅46 mm Tm:YAP crystal, and effectively overcomed the formation of defects such as cracking, dispersion, and verified that the diffuse scattering in YAP crystal has relationship with the temperature gradient and growth interface curvature.

In the present work we focus on the crystal growth of YAP at 2% doping level of Tm^{3+}. The formation mechanism of crystal defects is analyzed, and the crystal defects are reduced by annealing treatment. The segregation coefficient, concentration and absorption cross-section and other related parameters of crystal are calculated through analyzing the crystal absorption spectra.

1. EXPERIMENTAL

The source oxides Y_2O_3 (99.99%), Al_2O_3 (99.99%), and Tm_2O_3 (99.99%) were purchased from Science and Technology Parent Company of Changchun Institute of Applied Chemistry. Raw materials were dried in air at 200°C for 24 h, and then were calcined at 1000°C in Pt crucible for 2 h. The powders were mixed thoroughly and pressed into blocks at 500 kg/cm^2 pressure. The blocks' size was similar to the crucible diameter.

The Tm:YAP crystal was grown in an apparatus consisted of DJL-600 Czochralski furnace with conventional resistive heating, and the special care has been devoted to the quality of the vacuum system, which had an ultimate pressure limit better under 10^{-2} Pa. The growth process was carried out in a high purity (5N) nitrogen atmosphere. During the growth of Tm:YAP crystal, the rotation rate was ~15–25 rpm,

[1] The article is published in the original.

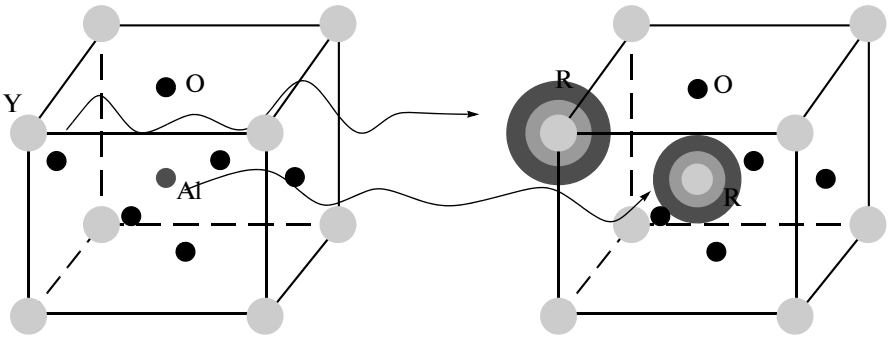

Fig. 1. Scheme of ion substitution.

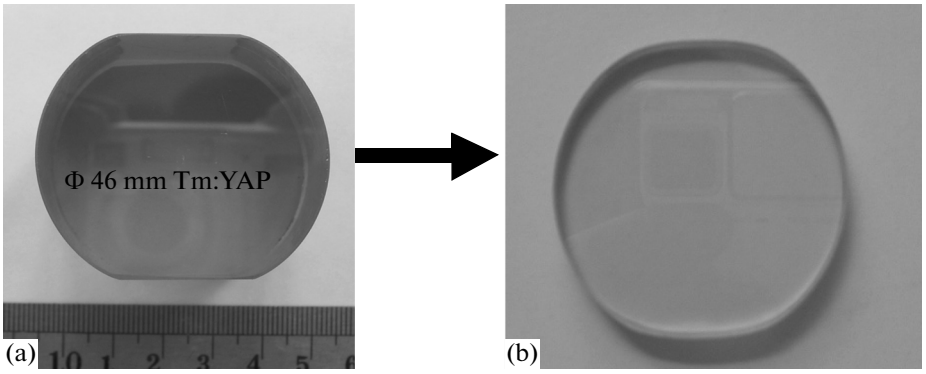

Fig. 2. Tm:YAP crystal before and after annealing.

and the pulling rate was ~1–2 mm/h. The obtained crystal was cooled down to room temperature at a rate of 20 K h^{-1}.

2. CRYSTAL ANNEALING

There were both external oxygen and interstitial ions of crystal itself filling in the vacancy while Tm:YAP crystal annealling in oxygen. The elimination speed of crystal color centers while annealing in oxygen was faster than that in argon, nitrogen or vacuum. Annealing in argon, nitrogen and vacuum relatively costs less and the process was easy to be operated. Annealing in hydrogen effect is relatively obvious, but it mainly affects absorption in ultraviolet and visible region. Its impact on the crystal absorption in infrared region was not great.

Annealing could reduce the color centers in Tm:YAP crystal. There was a distinct color change after annealing. YAP crystal's color was due to the fact that the low valence cation replaced the position of Y^{3+} or Al^{3+}, causing local charge imbalance in the crystal, and the changes of crystal color was caused by the influence of ion or vacancy migration around annealing on charge imbalance region, as shown in Fig. 1.

Tm:YAP crystal was annealed under the condition of vacuum with the following parameters: pressure ≤10 Pa; temperature rate is ~50–100 K h^{-1}; constant temperature is ~1000–1300°C; constant temperature time is 24 h. After Tm:YAP wafers were annealed, crystal color changed from red brown to colorless, as shown in Fig. 2, according to the test result of

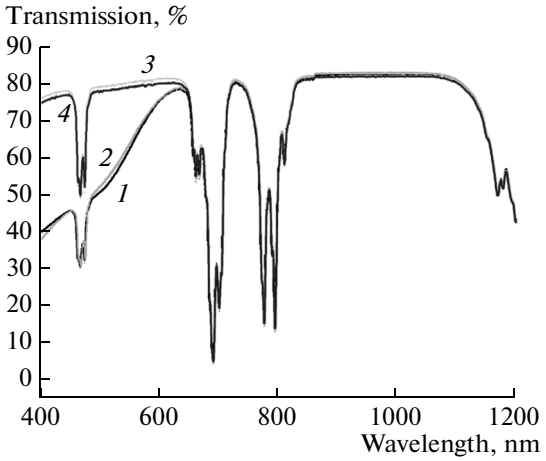

Fig. 3. Transmission spectrum of Tm:YAP crystal.

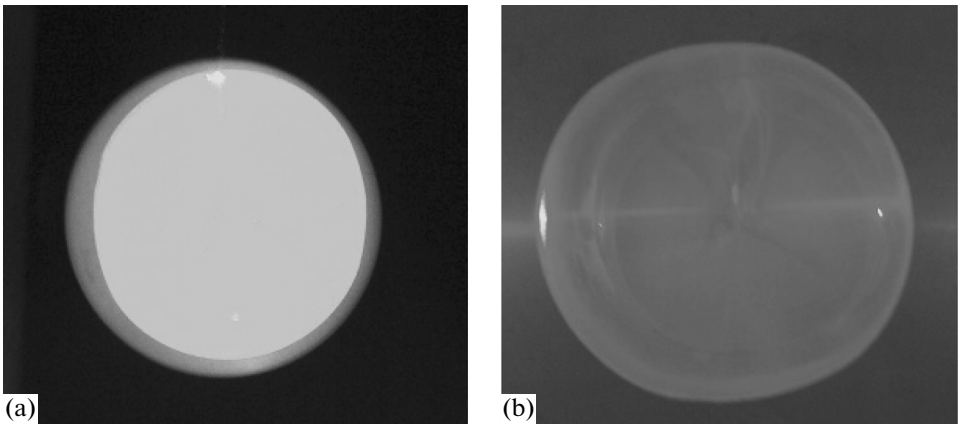

Fig. 4. Tm:YAP cloud layer defects of YAP crystal.

Kalaycioglu, Matkovskii, et al. [10]. Figure 3 shows a comparison of the transmission spectra of Tm:YAP crystal around annealing (*1*, *3* are crystal upper wafers, *2*, *4* are crystal lower wafers). From the Fig. 3, there is obvious color center absorption before annealing in the region of $\lambda < 650$ nm. The transmission rate is increased significantly after annealing. It indicates that after crystal annealing, the color center absorption in the ultraviolet and visible spectral region is effectively reduced. Thus the vacuum annealing is not only effective in reducing the crystal defects, but also is simply and safer than H_2 annealing.

3. DEFECT ANALYSIS

The clouds in Tm:YAP crystal have a severe impact on its optical quality (as shown in Fig. 4). The clouds is aggregation of small light scattering particles. It is very hard to overcome the problem completely. Firstly, the impurities in the raw materials for crystal growth are the causes of scattering defects. Secondly, the deviation of stoichiometry is another factor to cause clouds defects. The requirement of raw material ratio of Tm:YAP crystal is relatively high. If the component is partial to Y_2O_3, it may lead to $Y_4Al_2O_9$ (YAM) impurity phase formation in the growing crystal. If the component is partial to Al_2O_3, it may lead to $Y_3Al_5O_{12}$ (YAG) formation. The existence of miscellaneous phases is an important factor leading to the clouds dispersed point.

In addition, the rare earth ions removed from the solution side on solid-liquid interface of the crystal growth process, which may cause density, the growth diameter of crystal more great and the rare earth ion concentration density more easily came out. It may cause the supercooling growth and the serious clouds easily. Solid particles are continuously mixed into crystal during the process of crystal growth, which is the main reason for the formation of the scattering particles. The furnace temperature fluctuations greatly affect the process of crystal growth, and the rapid crystal rotation or seed loosening possibly cause scattering particle increasing in crystal.

While illumination of the obtained crystal with 532 nm, 45 mW green light laser, it can be seen from the end face that "light" appeared in the crystal, caused by the diffuse scattering, as shown in Fig. 5. Clouds are the large number of small scattering particles. They are caused by carbon and iron impurities in raw materials. Carbon impurities react with Al_2O_3 giving Al_4C_3. Therefore we proposed to eliminate the diffuse scattering by melt overheating and yttrium rich formula. Iron ions in the YAP structure exist as Fe^{2+} and Fe^{4+}, which need charge compensation, while the charge compensation is bound to causing color center defects. Adopting the high purity of ingredients, the problems of melt superheating, yttrium rich formula and diffuse scattering have not been resolved. It can be seen from Fig. 5, the center portion of the crystal cross-section does not give light scattering. Both ends have obvious scattering, and the diffuse scattering in the lower end is lighter than it in the upper end of crystal. It indicates that the formation of diffuse scattering is not only due to the influence of carbon impurities in raw materials, but also possibly related to the curvature of growth interface and temperature gradient. Further studies on crystal growth reveal that when the diameter of crystal growth increased gradually from 40 to 45 mm, the crystal growth gradually can be dominant by the forced convection. Diffuse scattering in crystal was significantly reduced, as shown in Fig. 5b. Increasing the crystal diameter can help reduce the diffuse scattering in YAP crystal.

The clouds and defects in Tm:YAP crystals are formed easily, which seriously restricts the performance of Tm:YAP crystal. Sugak et al. [11] argued that small scattering particles were caused by carbon or iron impurities in raw materials. The rules for formation mechanism of color centers and clouds defects in

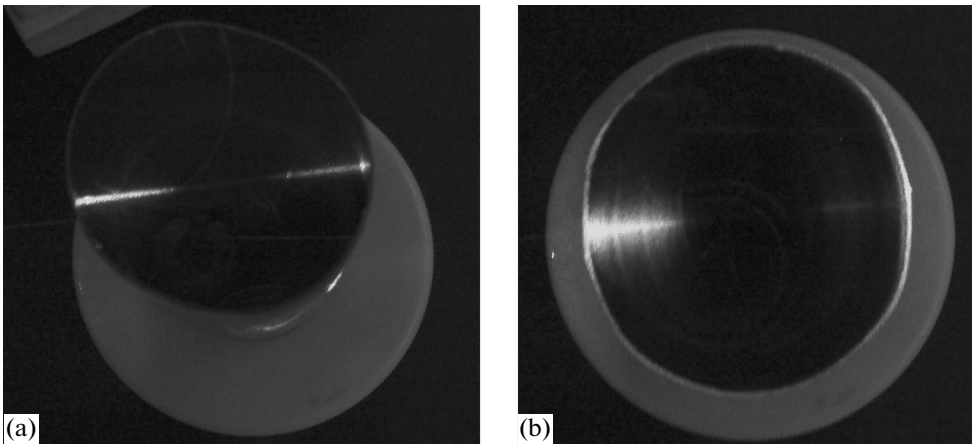

Fig. 5. Photos of crystal with clear diffusing scattering and notably reduced scattering.

crystal are summarized, and Tm:YAP crystal growth and annealing process are improved. The following recommendations can be formulated:

(1) Firstly, ensure the purity of raw materials: select 99.99% high purity of raw material; reduce the chance and time of raw materials touching outside in the production process, in strict accordance with the stoichiometric ratio of $Y_2O_3 : Al_2O_3 = 1 : 1$.

(2) Adjust crucible, the position and shape of stay-warm case to ensure the symmetry; adopt insulation measures around the crucible mouth to prevent cold air flow from impacting the liquid level of the crucible mouth; establish stable and reasonable space temperature field distribution. Strengthen the insulation effect and high insulation level; change the temperature gradient within the crystal interface above and reduce the temperature gradient melt above by high temperature heat radiation. Through providing a suitable and stable temperature field, a small temperature gradient is formed to control the heat transport.

(3) Crystal captures the solid-liquid interface inert solid particles, which can only be occurred as crystal growth rate is more than a "critical speed," and the "critical speed" relates to melt viscosity, solid particle properties and geometry. So this paper adopts low crystal transformation method to make the crystal growth rate much smaller than the "critical speed." On this account the crystal growth rate fluctuation can be reduced, and the shape of solid-liquid interface and stability of the interface can be controlled. Thereby the number of scattering particles and light dispersion point can be reduced.

(4) Adopt automatic temperature control of the Czochralski technique, to minimize temperature fluctuation, and reduce the change of crystal instantaneous growth rate caused by temperature fluctuation, which can lead to supercooling or inert solid particles.

4. ABSORPTION SPECTRA

The absorption spectra of Tm:YAP crystal in the range from 400 to 1200 nm were measured using Lambda900 spectrophotometer. There are three main absorption peaks located at 468, 694, and 794 nm, respectively (Fig. 6). The 694 and 794 nm absorption peaks correspond to Tm^{3+} induced transition from the $^3H_6$ state to the $^3F_3$, $^3H_4$ excited states. As can be seen from the absorption spectra, the peak at 694 nm is the strongest, and the peak at 794 nm matches with the excitation wavelength of InGaAs (~792–795 nm) laser diode pumping source. Therefore 794 nm is usually used pump wavelength for Tm:YAP crystal.

5. CRYSTAL PARAMETERS CALCULATION

We cut a test piece from both ends of the Tm:YAP crystal, and calculate concentration, distribution coefficient, absorption cross section and the crystal spectral properties. The transmittance at 794 nm was

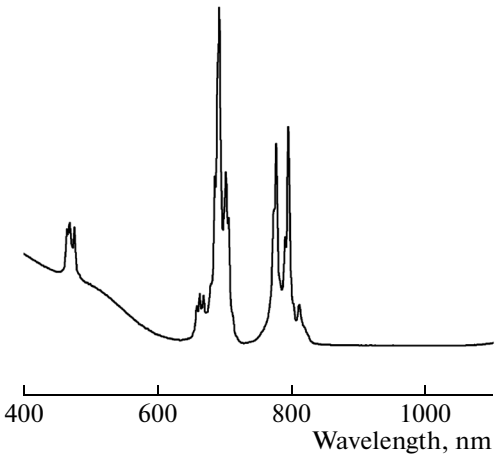

Fig. 6. Absorption spectrum of Tm:YAP crytal.

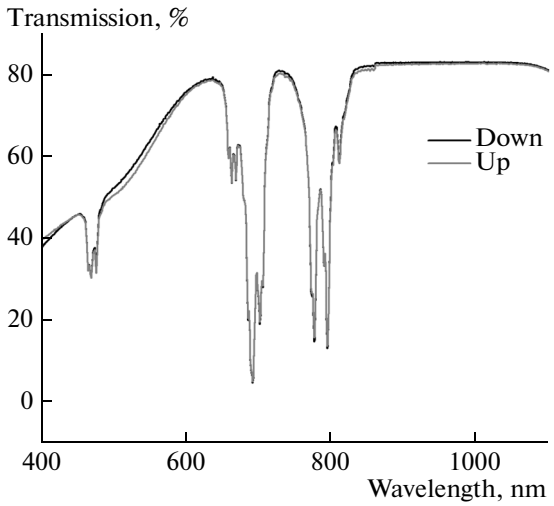

Fig. 7. Transmission spectrum of Tm:YAP crystal.

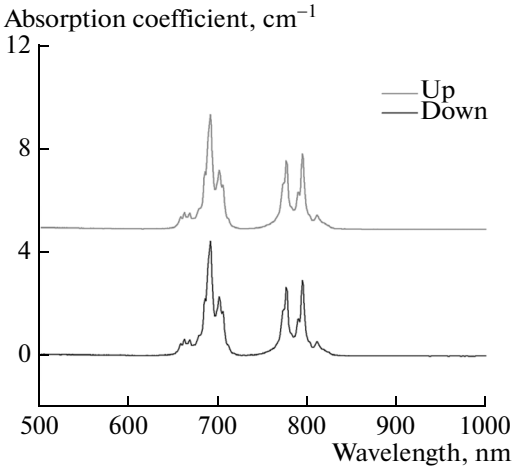

Fig. 8. Absorption coefficient curve of Tm:YAP crystal.

tested, and the transmittance of upper and lower part in crystal are $T_{up} = 13.36\%$ and $T_{down} = 13.31\%$, respectively.

The transmission rate and crystal residual emission rate formula are as follows:

$$T = \frac{I}{I_0} = e^{-\alpha d} \text{ and } R = \frac{(n-1)^2}{(n+1)^2} \text{ can obtain}$$

$$\alpha = \frac{\ln\dfrac{(1-R)^2}{T}}{d}. \quad (1)$$

In the formula, I is the light intensity after pass through the sample; I_0 is the light intensity before the sample; d is the thickness of the sample; α is the absorption coefficient.

The absorption coefficient curve can be obtained by taking the refractive index ($n = 1.923$) into formula (1), as shown in Fig. 8. The crystal absorption coefficient of up and down part are respectively $\alpha_{up} = 2.918$ cm^{-1} and $\alpha_{down} = 2.927$ cm^{-1}.

According to the diffusion formula, crystal at constant drawing speed condition, the relationship between the rare earth ions concentration in crystal C_c and in melt C_m:

$$C_c = k_{eff} C_m(0)(1-g)^{k_{eff}-1}. \quad (2)$$

In the formula, $C_m(0)$ is ion concentration in the initial melt; k_{eff} is effective segregation coefficient; g is the crystallization rate ($g = m_l/m_L$), m_l is t time crystal quality, m_L is the total mass of the melt; absorption cross section is $\sigma_{abs} = \dfrac{\alpha}{N_c}$, α is the absorption coefficient, $\alpha_c(l) = k_{eff}\alpha_m(0)(1 - m_l/m_L)^{k_{eff}-1}\left(\dfrac{\rho Na}{\mu}\right)$. Count the logarithm of both sides:

$$\ln\alpha_c(l) = (k_{eff}-1)\ln(1 - m_l/m_L) + \ln k_{eff} + \ln\alpha_m(0) + \ln\left(\frac{\rho Na}{\mu}\right), \quad (3)$$

$\alpha_c(l)$ changes with g; $\ln\alpha_c(l)$ and $\ln(1 - m_l/m_L)$ are in a linear relationship; the slope is $(k_{eff} - 1)$.

Figure 8 shows the transmittance and absorption coefficient of upper and lower parts of the crystal at 794 nm: $T_{up} = 13.36\%$, $\alpha_{up} = 2.918$ cm^{-1}, $T_{down} = 13.31\%$, $\alpha_{down} = 2.927$ mm^{-1}. The doping concentration is 2.5 at %; crystal density is $\rho = 5.35$ g/cm^3. $\sigma_{abc\perp} = 6.029 \times 10^{-21}$ cm^2, $\sigma_{abc\perp} = 6.045 \times 10^{-21}$ cm^2 can be calculated by taking them into the formula. The absorption cross section of $^3H_6 \longrightarrow {}^3H_4$ transition is 6.7×10^{-21} cm^2 which has little difference with what Kalaycioglu [10] states. It shows that the obtained laser crystal has great characteristics.

CONCLUSION

Tm:YAP crystal is grown by the Czochralski method, and annealed in vacuum of ≤10 Pa at 1000–1300°C for 24 h. Temperature increase rate was 50–100 K h^{-1}. After crystal annealing, the absorption in the ultraviolet and visible range was effectively reduced. While forced convection is dominant, the diffuse scattering in the crystal is significantly reduced, and diffuse scattering in Tm:YAP crystal reduces while crystal diameter is increased. The crystal absorption

coefficient and absorption cross-section are calculated to provide references for the Tm:YAP crystal characterization.

ACKNOWLEDGMENTS

This work was supported by the Science and Technology Department of Jilin Province (201215177). The authors also wish to thank Dr. Haiying Sun and Dr. Yunchun Wan for carrying out the tensile tests.

REFERENCES

1. A. Bensalah, K. Shimamura, Vikas Sudesh, et al., J. Cryst. Growth **223**, 539 (2001).
2. R. A. McFarlane, Opt. Soc. Am. B **11**, 871 (1994).
3. Chun Li, Xuejian Zhang, Chengwei Wang, et al., Chin. J. Inorg. Chem. **27**, 6 (2011).
4. K. S. Lai, P. B. Phua, R. F. Wu, et al., Opt. Lett. **25**, 1591 (2000).
5. N. I. Borodin, P. V. Kryukov, A. V. Popov, et al., Quantum Electron. **35**, 511 (2005).
6. P.-X. Song, Zh.-W. Zhao, X.-D. Xu, et al., J. Inorg. Mater. **20**, 869 (2005).
7. Gansheng Li, Xibin Guo, et al., J. Cryst. Growth **118**, 371 (1992).
8. Yang Yang, Yanling Lu, Jun Wang, et al., J. Alloys Compd. **455**, 1 (2008).
9. X.-G. Mo, Y.-G. Wang, J.-H. Zhu, et al., J. Synth. Cryst. **36**, 520 (2007).
10. H. Kalaycioglu, A. Sennaroglu, et al., IEEE J. Sel. Top. Quantum Electron. **11**, 667 (2005).
11. D. Sugak, A. Matkovskii, D. Savitskii, et al., Phys. Status Solidi A **184**, 239 (2001).